JOURNAL OF MATERIALS SCIENCE 10 (1975) 1334–1342

Failure of brittle polymers by slow crack growth

Part 1 *Crack propagation in polymethylmethacrylate and time-to-failure predictions*

PETER W. R. BEAUMONT, ROBERT J. YOUNG
Department of Engineering, University of Cambridge, UK

Slow crack growth in two forms of polymethylmethacrylate (PMMA) has been studied from a fracture mechanics viewpoint. It has been found that in Perspex acrylic sheet and surgical Simplex acrylic bone cement the crack velocity, V, for each material depends upon the intensification of stress at the tip of the crack. Experimental measurements have been made of V as a function of the stress intensity factor, K_I, at the crack tip, and a derived $V(K)$ relationship has been used to predict the times-to-failure of components made from Perspex and Simplex bone cement. Direct measurements of times-to-failure for Perspex are entirely consistent with the predicted values.

1. Introduction

The design of structural components requires a thorough knowledge of the properties of the engineering material and the pertinent failure criterion for that load-bearing member. A fracture mechanics approach is frequently used as a failure criterion for high strength materials and the plane strain fracture toughness, K_{IC}, defines the onset of brittle (unstable) fracture of the material. The fracture toughness, K_{IC}, of a material is dependent on the microstructural features and is generally insensitive to the chemical species in the surrounding environment. However, under certain stress and environmental conditions, imperfections or flaws in a structural material can slowly extend and lead to a time-dependence on fracture stress. The successful exploitation of the engineering material, therefore, requires a detailed understanding of the time-dependent failure characteristics of the material so that accurate failure predictions can be made.

Fracture involves two time-sensitive processes; (1) crack initiation and (2) crack propagation. The structural life-time of a component can, therefore, be considered simply as the sum of the times for completion of the two stages of fracture. This means that

$$\Psi_f = \Psi_i + \Psi_p \quad (1)$$

where Ψ_f is the time-to-failure, and Ψ_i and Ψ_p are the times to initiate and propagate a crack to some critical size, respectively, at which point catastrophic fracture occurs. Cracking can, therefore, commence at a value of $K_I < K_{IC}$, where K_I is the stress intensity factor describing the state of stress at the crack tip. (The subscript I refers to the crack opening mode of failure.) The threshold value of K_I at which cracking starts (designated K_I^*) depends to a large extent on the level of applied stress and the environmental conditions; it does not ordinarily rely entirely on the properties of the material. Under conditions leading to subcritical crack growth at $K_I < K_{IC}$, the dynamics of crack propagation can be described uniquely by the stress intensity factor, K_I, at the crack tip and a corresponding crack velocity, V, ($= da/dt$ under constant stress), shown schematically in Fig. 1. The curve may in general be divided into three regions of crack growth; regions I and II result from the effects of a stress and environment, whilst region III represents mainly mechanical failure and is essentially independent of the environment.

There is now a considerable body of information to support the idea of applying linear elastic fracture mechanics concepts to explain the time-dependent fracture behaviour of brittle

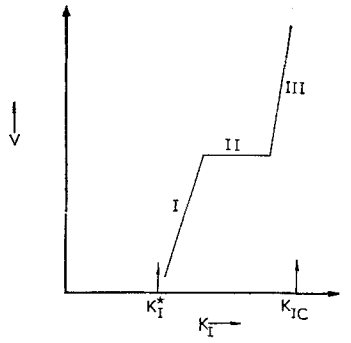

Figure 1 Schematic representation of a typical $V(K)$ diagram for a brittle solid exhibiting three stages of crack growth.

and semi-brittle polymers [1]. Predictions of fracture stress, therefore, require a knowledge of the kinetics of crack growth in terms of a $V(K)$ relationship, where V is the crack velocity. In this paper we have experimentally derived the $V(K)$ function for two types of polymethylmethacrylate (PMMA): (1) a commercial grade of PMMA manufactured by ICI Ltd, called Perspex; and (2) an acrylic bone cement called "surgical Simplex P" supplied in the form of PMMA powder and MMA liquid monomer by North Hill Plastics Ltd. We have constructed $V(K)$ diagrams to obtain information on the fracture characteristics and times-to-failure of the polymer as a function of applied stress (or stress intensity factor), temperature, and environment (water). The effect of small additions of spherical inclusions of polymethylmethacrylate-polystyrene co-polymer and barium sulphate on the fracture behaviour of Simplex bone cement has been discussed.

2. Experimental

2.1. Materials and environmental conditions

Two kinds of polymethylmethacrylate (PMMA) have been investigated; (1) cast sheet of Perspex, and (2) an acrylic bone cement (Simplex P). The acrylic bone cement contains small spherical particles of a polymethylmethacrylate-polystyrene co-polymer and up to 10% by weight of very fine barium sulphate inclusions. The Simplex cement was fabricated using a PMMA: MMA monomer ratio of 2:1. When the resulting dough had lost its tackiness, the acrylic cement was placed between two aluminium plates and compressed to a thickness of about 3 mm. A pressure of 700 kN m^{-2} was maintained on the sample until curing was complete and the heat generated began to diminish.

Crack growth tests were carried out in air at 20 ± 2°C with a relative humidity of 60 ± 10%, and in distilled water at the same temperature.

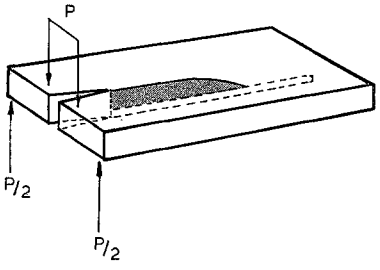

Figure 2 Schematic representation of the DT specimen and loading configuration. (The shaded area represents fracture surface.)

2.2. Specimen design and analysis

Subcritical crack growth has been monitored successfully using several experimental techniques in metals [2], ceramics [3, 4] and polymers [5, 6]. In this work, a double-torsion (DT) specimen is used [7] which consists of a rectangular plate (75 mm × 30 mm × 6 mm thick) containing an edge-notch at one end and a shallow centre-groove along one of the faces of the specimen. During the DT test, the sample is supported on two parallel rollers, with the centre-groove on the bottom face, and loaded using two hemispheres at the notched end (Fig. 2). A crack is forced to propagate at the root of the notch and is guided by the shallow groove (see the shaded portion in Fig. 2). It can be shown [7] that the stress intensity factor, K_I, at the crack tip is independent of crack length in the DT specimen and for an elastic material is given by:

$$K_I = PW_m \left[\frac{3(1+\nu)}{Wt^3 t_n}\right]^{\frac{1}{2}} \quad (2)$$

where P is the applied load, W_m is the moment arm, ν is Poisson's ratio, W is the bar width, t is the bar thickness, and t_n is the plate thickness in the plane of the crack. For PMMA, ν has been taken to be 0.33.

2.2.1. Constant displacement (load relaxation) method

If the plate is loaded and held at constant

displacement ($dy/dt = 0$), the crack growth rate ($da/dt = V$) is given by [7];

$$\frac{da}{dt} = V = -\frac{P_{i,f}}{P^2}\left(a_{i,f} + \frac{C}{B}\right)\left(\frac{dP}{dt}\right)_y \quad (3)$$

where $P_{i,f}$ is the initial (or final) load, P is the instantaneous load, $a_{i,f}$ is the initial (or final) crack length, and B and C are constants relating to the slope and intercept of a compliance analysis calibration curve for the DT specimen, $(y/P)\,f(a)$, respectively. The values of B and C were 1.1×10^{-4} N^{-1} and 1.3×10^{-3} mm N^{-1}, respectively, for Perspex, and 2×10^{-4} N^{-1} and 1.8×10^{-3} mm N^{-1}, respectively, for the Simplex acrylic bone cement.

The crack velocity can, therefore, be found directly from the rate of load relaxation $(dP/dt)_y$, providing the initial or final values of load ($P_{i,f}$) and crack length ($a_{i,f}$) are known, and providing the material does not suffer from mechanical relaxation due to, for example, molecular rearrangements in the arms of the DT specimen. This source of error can be reduced by pre-loading the sample to P^* (or K_I^*)† for about 30 min before carrying out the experiment. By this means, some of the molecular relaxation can be eliminated before carrying out the load relaxation test.

Observations of the crack front profile during crack propagation show that the crack extends further along the lower face than the upper face. The crack velocity is, therefore, smaller than given by Equation 3 by an amount determined by the ratio $\Delta a/b$ where Δa is the difference between the crack length measured along the top and bottom faces of the DT specimen, and b is the width of the crack [7]. Thus, Equation 3 becomes;

$$V = -\phi\frac{P_{i,f}}{P^2}\left(a_{i,f} + \frac{C}{B}\right)\left(\frac{dP}{dt}\right)_y \quad (4)$$

where $\phi = b/(\Delta a^2 + b^2)^{\frac{1}{2}}$. For 6 mm thick PMMA ϕ equals 0.4. At any particular value of crack velocity, the stress intensity factor may be calculated from the instantaneous load, P, and specimen dimensions using Equation 2.

2.2.2. Constant load method

If the plate is loaded to a constant load ($dP/dt = 0$), the crack growth rate can be calculated providing the initial and final values of crack length ($a_{i,f}$) are known and also the time interval between obtaining these two measured values, i.e. $V = (\Delta a/\Delta t)_P$. The stress intensity factor may be calculated from the constant applied load, P, using Equation 2. This experimental approach is particularly useful for obtaining $V(K)$ information at low crack speeds in visco-elastic materials and, therefore, the test method can be repeated several times on the same specimen. The load relaxation method for visco-elastic materials can lead to erroneous results at long times (low values of crack velocity) and, therefore, this latter approach provides a check on the former method as well as obtaining crack velocities as a function of K_I.

2.2.3. Constant displacement rate method

Under constant displacement rate conditions, (dy/dt) = constant, the crack propagates at a constant load, P, (or K_I). It can be shown [7] that

$$\left(\frac{dy}{dt}\right) = BP\left(\frac{da}{dt}\right) = BPV \quad (5)$$

where B is a constant related to the slope of a compliance calibration curve for the material.

2.2.4. Time-to-failure (ψ_f)

In many structural materials (for a given environment, temperature), there exists a unique relationship describing the crack growth rate in terms of the stress intensity factor at the crack tip. The crack velocity, V, is generally expressed as a power function of K;

$$V = AK^n \quad (6)$$

where A and n are system constants. The time-to-failure, ψ_f, can easily be obtained from the above equation and the definition of stress intensity factor, $K_I = Y\sigma_a\sqrt{a}$, where σ_a is the gross applied stress, a is the length of a surface crack, and Y is a geometrical constant equal to $\sqrt{\pi}$ for small cracks in infinitely large plates;

$$\psi_f = \frac{2}{Y^2\sigma_a^2}\int_{K_{Ii}}^{K_{If}}\frac{K_I}{V(K_I)}\,dK_I \quad (7)$$

$$= \frac{2[(K_{Ii}^{2-n} - K_{If}^{2-n})]}{[(n-2)A\,Y^2\sigma_a^2]}. \quad (8)$$

If we assume instantaneous fracture to occur when the final stress intensity factor, K_{If}, reaches K_{IC}, then the time-to-failure is given by:

†P^* (or K_I^*) is the value of load (or stress intensity factor) below which no crack growth can be observed ($V < 10^{-10}$ m sec^{-1}).

$$\psi_f = \frac{2[(K_{Ii}^{2-n} - K_{IC}^{2-n})]}{[(n-2)AY^2\sigma_a^2]}. \quad (9)$$

If n is large and $K_{Ii} < 0.9\,K_{IC}$, Equation 8 can be written approximately as:

$$\psi_f \cong \frac{2K_{Ii}^{2-n}}{[(n-2)AY^2\sigma_a^2]}. \quad (10)$$

3. Results and discussion

3.1. $V(K)$ relationships

Slow crack growth has been observed in Perspex and Simplex cement. Tests were carried out in air and water at 20 ± 2°C to study the stable, subcritical crack growth under potentially hostile environments. The relationships between V and K determined for the two forms of PMMA are shown in Figs. 3 and 4. Included in Fig. 3 are the data from Marshall *et al.* [6] results on Perspex at room temperature. With the inclusion of Marshall's data, the room temperature curve has a similar shape to the idealized curve shown in Fig. 1 showing a transition at $V \cong 10^{-3}$ m sec^{-1}. Region III occurs at K_I values approaching K_{IC} and we will assume for purposes of time-to-failure prediction that fast fracture occurs when K_I equals K_{IC}. We can see that regions I and II can be described by the expression in Equation 6 and the value of n (slope of the line) for stage I cracking is 25 ± 2 for both Perspex and Simplex, and for stage II cracking in Perspex, n equals 12 ± 1. Although both curves are similar in shape for stage I cracking, $n = 25$, they differ in position along the K_I axis. The data for Simplex shows K_{IC} close to 1.8 (± 0.1) MN m$^{-3/2}$ compared with K_{IC} for Perspex equal to 1.6 (± 0.1) MN m$^{-3/2}$ in air. There is no apparent indication of a stress corrosion limit (K_I*) but extrapolation of the $V(K)$ curve for Perspex in air down to about 10^{-10} m sec^{-1}, (essentially no measurable crack growth), gives a corresponding K_I value of about 0.6 MN m$^{-3/2}$ which is close to the value of K_I of 0.65 MN m$^{-3/2}$ reported [8] for craze initiation in Perspex. The proposed model for crack initiation, therefore, requires a critical stress, σ_0, at the crack tip to nucleate a craze shown [8] to be equal to 8.1 × 10^7 N m^{-2}. This value of σ_0 (or K*) must not be considered a material property since it is both a function of

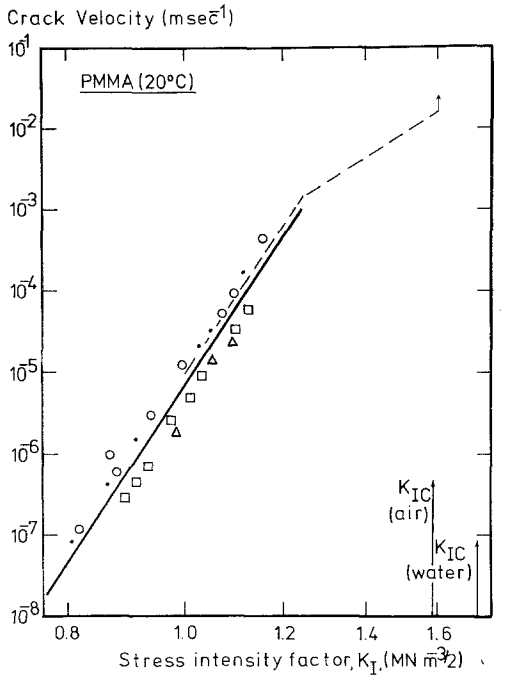

Figure 3 A $V(K)$ diagram for Perspex acrylic sheet in air at 20°C. The different symbols indicate separate specimens. ● and △ refer to optical measurements of crack velocity; □ and ○ indicate crack velocity measurements made using the load relaxation method. (The dashed line indicates the data of Marshall *et al.* [6]).

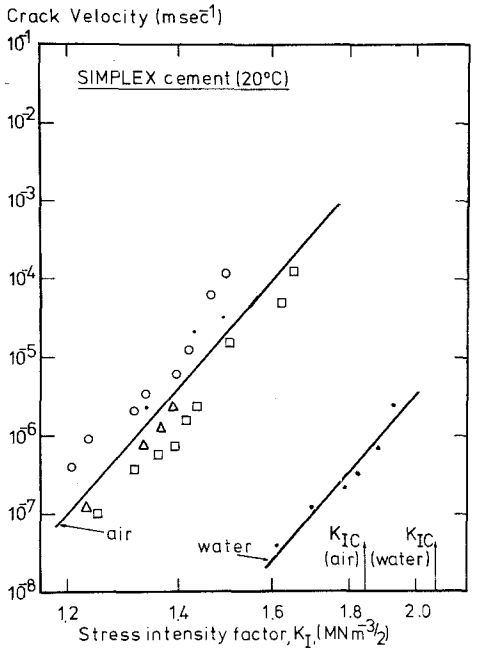

Figure 4 $V(K)$ diagrams for Simplex acrylic bone cement in air and water at 20°C. The different symbols refer to separate specimens. □ and ○ indicate crack velocity measurements made using the load relaxation method; ● and △ refer to optical measurements of crack velocity.

the material and the environment, and indications are that crazing in polymers is dependent on time (strain-rate), temperature, and environment.

The value of n for Simplex cement (Fig. 4) is unaffected by distilled water as would be expected since the slope n is related to the activation volume for the stress enhanced environment polymer reaction [11]. The constant A (Equation 6) for Simplex, however, is affected by water [9], and for Perspex, by temperature [6]. For Perspex, water appears to eliminate completely any slow crack growth at $K_I < K_{IC}$ and the fracture toughness, K_{IC} is slightly increased to 1.7 ($\pm$ 0.1) MN m$^{-3/2}$. Large "bunches" of crazes were observed at the crack tip as soon as the Perspex was loaded in water. This water-induced plasticized zone ahead of the crack tip effectively blunts out the propagating crack by absorbing the stored elastic strain energy in the specimen that would have been dissipated as fracture surface energy. The fracture toughness, K_{IC}, of the Simplex cement is raised to 2.1 ($\pm$ 0.1) MN m$^{-3/2}$ by exposing to water. We conclude that water plasticization of PMMA at the crack tip is the reason for this increase in toughness.

The accuracy of the $V(K)$ data may be appreciated by comparing times-to-failure, ψ_f, at constant stress predicted using the $V(K)$ diagrams with measured times-to-failure in the next section.

3.2. Time-to-failure predictions

The relationship between V and K can be used for purposes of fracture-safe design in situations where the life-time of a component is determined by sub-critical (stable) crack growth. It has been shown that in Perspex and Simplex, the crack growth rate (V) is a unique function of K_I and, therefore, from a knowledge of the material's fracture toughness, K_{IC}, and working stress, σ_w, (or K_{Ii}), we can calculate the time-to-failure of the component in question as a function of σ_w/σ_f (or K_{Ii}/K_{IC}), or fracture stress as a function of time. From the definition of stress intensity factor, the ratio K_{Ii}/K_{IC} can be shown to be equal to a_i/a_{IC} or a_0/a_{IC} at constant stress, where a_i is initial crack size, a_0 is the inherent flaw size in the material, and a_{IC} is the critical crack size for a given working stress. The time-to-failure, ψ_f, at constant stress is simply the integral of the $V(K)$ function. As shown in Fig. 3, the $V(K)$ curve shows two regions of slow (stable) crack growth at $V < 1$ m sec^{-1}; in region I, $V \propto K^{25}$; in region II, $V \propto K^{12}$. It is convenient, therefore, to separate the integral of $V(K)$ relationships into two parts;

$$\psi_f = \frac{2}{\sigma^2 Y^2}\left(\int_{K_I^*}^{K_t} \frac{K_I}{V(K_I)}\,dK_I + \int_{K_t}^{K_{IC}} \frac{K_I}{V(K_I)}\,dK_I\right) \tag{11}$$

where the first integral refers to stage I cracking and the second integral refers to stage II cracking. K_t is the value of K_I at the transition between stage I and stage II.

Since region II occurs at a high crack velocity ($V_t = 10^{-3}$ m sec^{-1} at K_t), the time-to-failure is controlled essentially by region I cracking except at very short times ($t \ll 1$ sec). This equation is plotted for Perspex at room temperature using an applied stress, σ_a, equal to 2.7 MN m^{-2}, Y equal to 4 and K_{IC} equal to 1.62 MN m$^{-3/2}$ (Fig. 5).

The solid points in Fig. 5 are experimental time-to-failure data for single-edge cracked tensile specimens (25 mm wide) loaded to a value of σ_a of 2.7 $\pm$ 0.1 MN m^{-2}. The edge-cracks were between 9 and 13 mm long giving a range of values of stress intensity factor (K_{Ii}). For the ratios of crack size: specimen width chosen, the geometrical constant, Y, was of the order of 4. The measured data show a high degree of scatter but within experimental error it can be seen that all the points lie on or to the right of the theoretical prediction. It shows that it is possible to integrate the $V(K)$ function and obtain a conservative estimate of the life-time of the component. At any particular value of $K_I < K_{IC}$, failure occurs after an incubation period that can either be accounted for as the time for crack initiation or as a function of the crack growth kinetics as we have shown. We have, therefore, presented a conservative fracture-safe design prediction by ignoring the possibility of a finite crack initiation time ($\psi_i = 0$).

The scatter in experimental results is probably due to the variation in crack tip geometry caused by the notching procedure. Atomically "sharp" cracks were obtained by slowly pushing a razor blade into the bottom of a saw-cut and it was noticed that in some cases the cracks tended to bifurcate although such samples were generally discarded.

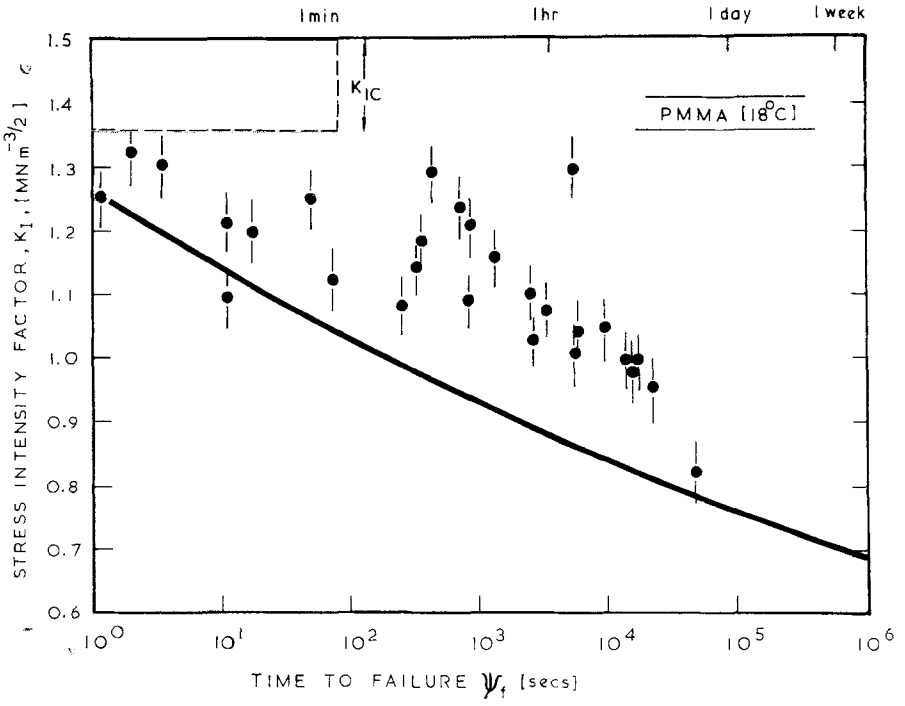

Figure 5 Experimental time-to-failure data for single edge cracked Perspex acrylic sheet tensile specimens as a function of initial stress intensity factor. (The solid curve shows the predicted ψ_f values.)

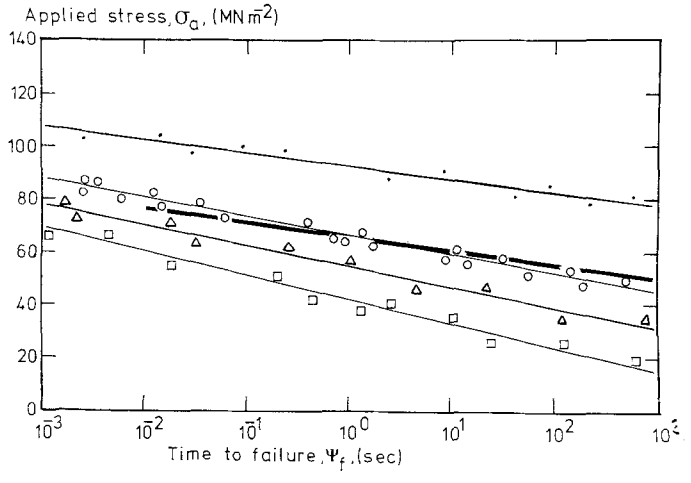

Figure 6 A strength-time diagram for unnotched Perspex acrylic sheet as a function of temperature [10], where ● = − 23°C, ○ = 18°C, △ = 50°C and □ = 70°C. (The solid line shows the predicted ψ_f values for 20°C.)

Equation 7 may also be used to construct $\sigma_f(t)$ diagrams and estimate the inherent flaw size, a_0, of the material. Some strength data of Zhurkov [10] is available (Fig. 6) and we can, therefore, evaluate a_0 before constructing $\sigma_f(t)$ curves.

The inherent flaw size, a_0, can be evaluated by fitting the $V(K)$ function to Zhurkov's room temperature data [10] using Equation 7. At σ_a = 67 MN m^{-2} the time-to-failure, ψ_f, is 1 sec. If we assume that $Y = \sqrt{\pi}$ for very small values of a_0, and K_{IC} = 1.62 MN m$^{-3/2}$, it is possible to solve for K_{Ii}; a_0 is then simply equal to $(1/\pi)\,(K_{Ii}/\sigma_a)^2$. The inherent flaw size of Perspex at 20°C was found to be equal to 0.073 ± 0.004 mm which compares favourably with Berry's value [12]

(see Table I). The room temperature data covers regions I and II cracking and the agreement with Zhurkov's experimental results is evidence for the validity of the test method and the usefulness of $V(K)$ diagrams for predicting times-to-failure. A prediction of strength at short times for Perspex at different temperatures is shown in Fig. 7, using the $V(K)$ relationship obtained by Marshall *et al.* [6] and values of a_0 listed in Table I. It can be seen that for each temperature there are two kinds of behaviour; at high stresses close to the fracture stress, the time-

TABLE I The inherent flaw size (a_0) of PMMA as a function of temperature [12]

a_0 (mm) $\pm$ 0.05 mm	Temperature (°C)
0.075	− 60
0.067	− 40
0.062	− 20
0.066	0
0.075	20
0.095	40
0.12*	60
0.15*	80

*by extrapolation of Berry's data.

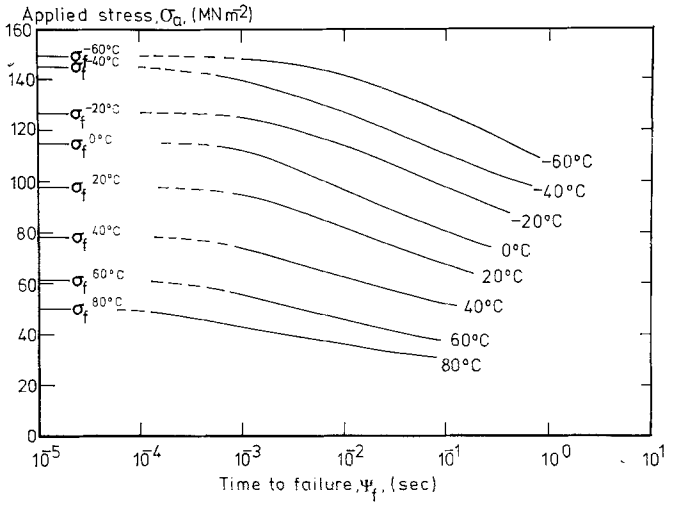

Figure 7 A prediction of strength for Perspex at short times as a function of temperature, using Marshall *et al.*'s [6] data and the inherent flaw sizes, $a_0 f(T)$ obtained by Berry [12].

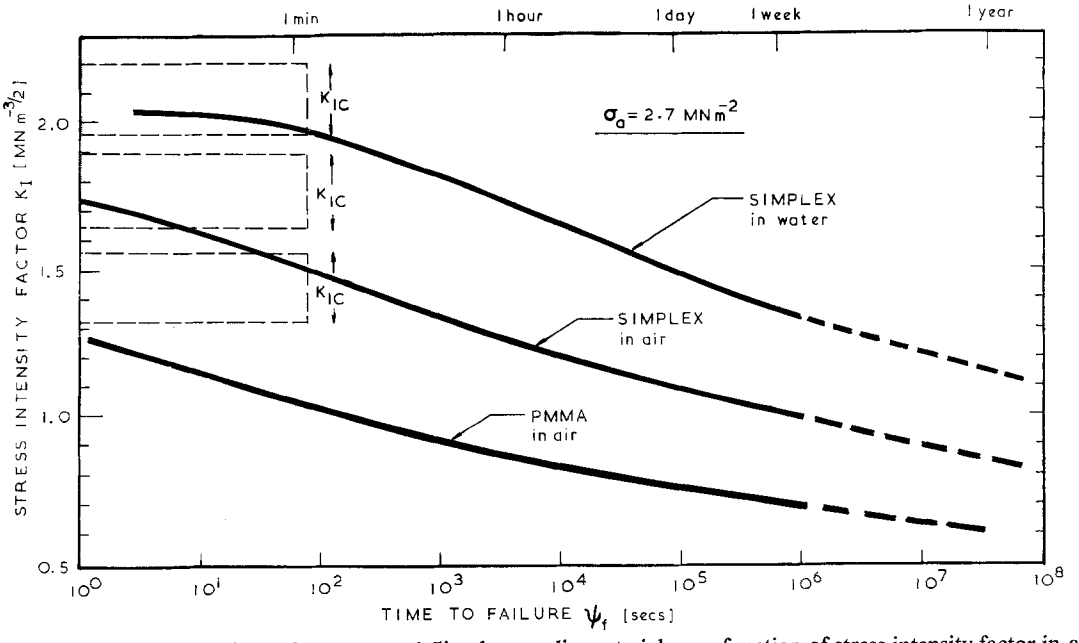

Figure 8 Predicted ψ_f values of Perspex and Simplex acrylic materials as a function of stress intensity factor in air and water at 20°C.

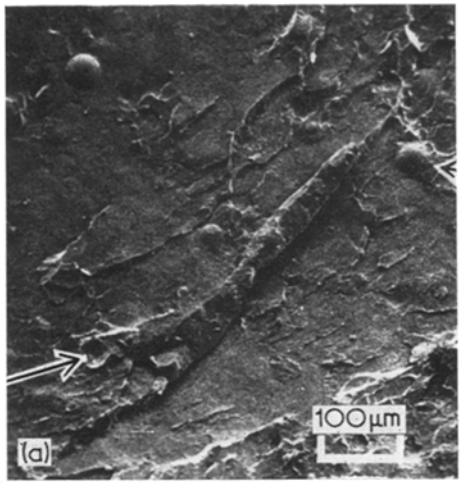

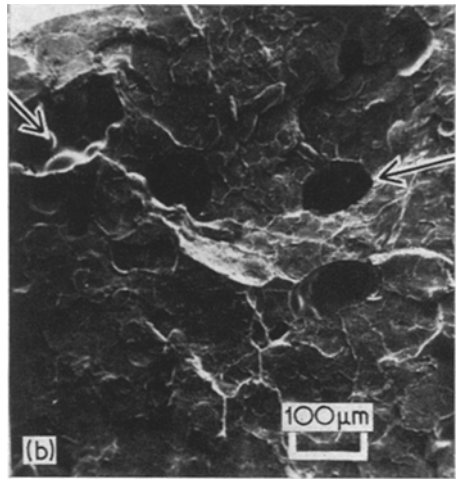

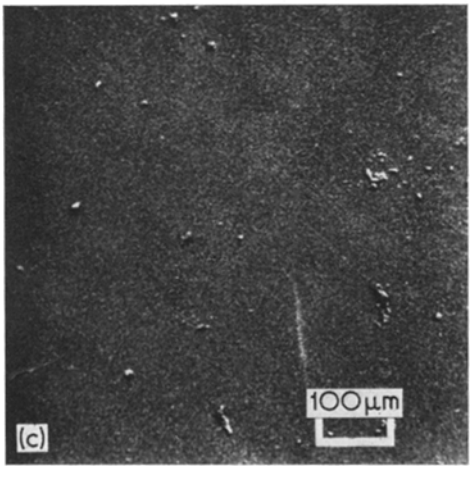

Figure 9 Scanning electron microscopic photomicrographs of the fracture surfaces of (a) and (b) Simplex acrylic bone cement and (c) Perspex. (a) Arrows: top right, PMMA particle; bottom left, crater left by pulled out PMMA particle. (b) Arrows: left, void containing PMMA particles; right, void.

to-failure is extremely sensitive to small changes in stress; secondly, over an intermediate stress range (which is temperature dependent) the failure time is less sensitive to changes in stress. The transition between the two types of behaviour occurs at shorter times as the temperature decreases.

The analytical derived curves shown in Fig. 8 illustrate the usefulness of the stress intensity factor for comparing the behaviour of the two kinds of PMMA. The time-to-failure curves were plotted using Equation 7 for σ_a equal to 2.7 MN m^{-2} and Y will depend on the crack size and component geometry. For a particular value of K_{Ii} the structural life-time of Simplex is about three decades of time greater than for Perspex (at constant stress). The dashed lines are extrapolations of the time-to-failure curves assuming that the $V(K)$ curves may be extrapolated to lower velocities. In order to obtain time-to-failure data over periods of months or years, it is necessary to measure crack velocities of 10^{-10} m sec^{-1} or less.

3.3. Scanning electron microscopy

Fracture surfaces of both Perspex and Simplex cement were examined in a Stereoscan scanning electron microscope. The surfaces were prepared for examination by depositing thin layers ($\sim$ 100 Å thick) of carbon and gold-palladium alloy on to the fracture surfaces. Fig. 9a and b shows fracture surfaces of Simplex cement in air. The surface is rough and spherical particles of PMMA can be seen protruding from it. There are also areas containing spherical pits where particles have been pulled out during crack propagation. In other areas there are voids that were caused by trapped pockets of air or monomer during the fabrication of the Simplex cement [9]. This can be contrasted with the Stereoscan photomicrograph of a Perspex fracture surface (Fig. 9c) at approximately the same magnification which appears to be "perfectly" smooth.

Fig. 9a and b shows a mixed mode of failure in the Simplex cement with areas of transparticle and interparticle fracture. In interparticle failure, the slowly moving crack has followed paths of weakness between spherical PMMA particles that have not completely polymerized together.

This mode of failure may account for the rougher fracture surface appearance of the Simplex cement compared to that of PMMA, although crack propagation through the strongly-bonded areas also produces a fairly irregular fracture surface. At the present time, we do not know the effect of the micro-fine particles of barium sulphate on the fracture characteristics of the Simplex cement. Paradoxically, it appears that the Simplex cement is strengthened against cracking by these weak interfaces between PMMA spheres which causes the crack front to deviate during crack progression. This is a possible explanation for the displacement of the $V(K)$ curve for Simplex cement to the right of the curve for Perspex, i.e. at a particular value of $K_I < K_{IC}$, the crack moves more slowly through the bone cement than in Perspex. In terms of energy, at a particular crack velocity, the crack driving force is greater in Simplex than in Perspex.

4. Conclusions

A technique developed for measuring sub-critical crack growth in brittle materials has been used successfully in determining $V(K)$ diagrams for Perspex and Simplex bone cement in air and water. The excellent agreement between experimentally measured time-to-failure and values of ψ_f predicted in air using the $V(K)$ diagram strengthens the validity of this approach for investigating crack growth phenomena in these kinds of materials.

Acknowledgements

We are grateful to Mr L. Shadbolt of North Hill Plastics Ltd for supplying us with the Simplex surgical cement. One of us (R.J.Y.) would like to thank the Master and Fellows of St. John's College, Cambridge for support in the form of a Research Fellowship.

References

1. R. P. KAMBOUR, *J. Polymer Sci. Macromol. Rev.* **7** (1973) 1.
2. H. G. NELSON, A. S. TETELMAN and D. P. WILLIAMS, Proceedings of the International Conference on Corrosion Fatigue, Storrs, Connecticut, June (1971).
3. S. M. WIEDERHORN, *J. Amer. Ceram. Soc.* **50** (1967) 407.
4. A. G. EVANS, *J. Mater. Sci.* **7** (1972) 1137.
5. J. G. WILLIAMS and G. P. MARSHALL, *Proc. Roy. Soc.*, to be published.
6. G. P. MARSHALL, L. H. COUTTS and J. G. WILLIAMS, *J. Mater. Sci.* **9** (1974) 1409.
7. A. G. EVANS, *Int. J. Fracture* **9** (1973) 267.
8. H. R. BROWN and I. WARD, *Polymer* **14** (1973) 469.
9. P. W. R. BEAUMONT and R. J. YOUNG, *J. Biomed. Mats. Res.*, to be published.
10. S. N. ZHURKOV, *Int. J. Fracture Mechs.* **1** (1965) 311.
11. F. BUECHE, "Physical Properties of Polymers", (Interscience, New York, 1962), Ch. 11.
12. J. P. BERRY, in "Fracture Processes in Polymeric Solids", edited by B. Rosen (Interscience, New York, 1964) Ch. II.

Received 31 December 1974 and accepted 13 January 1975.